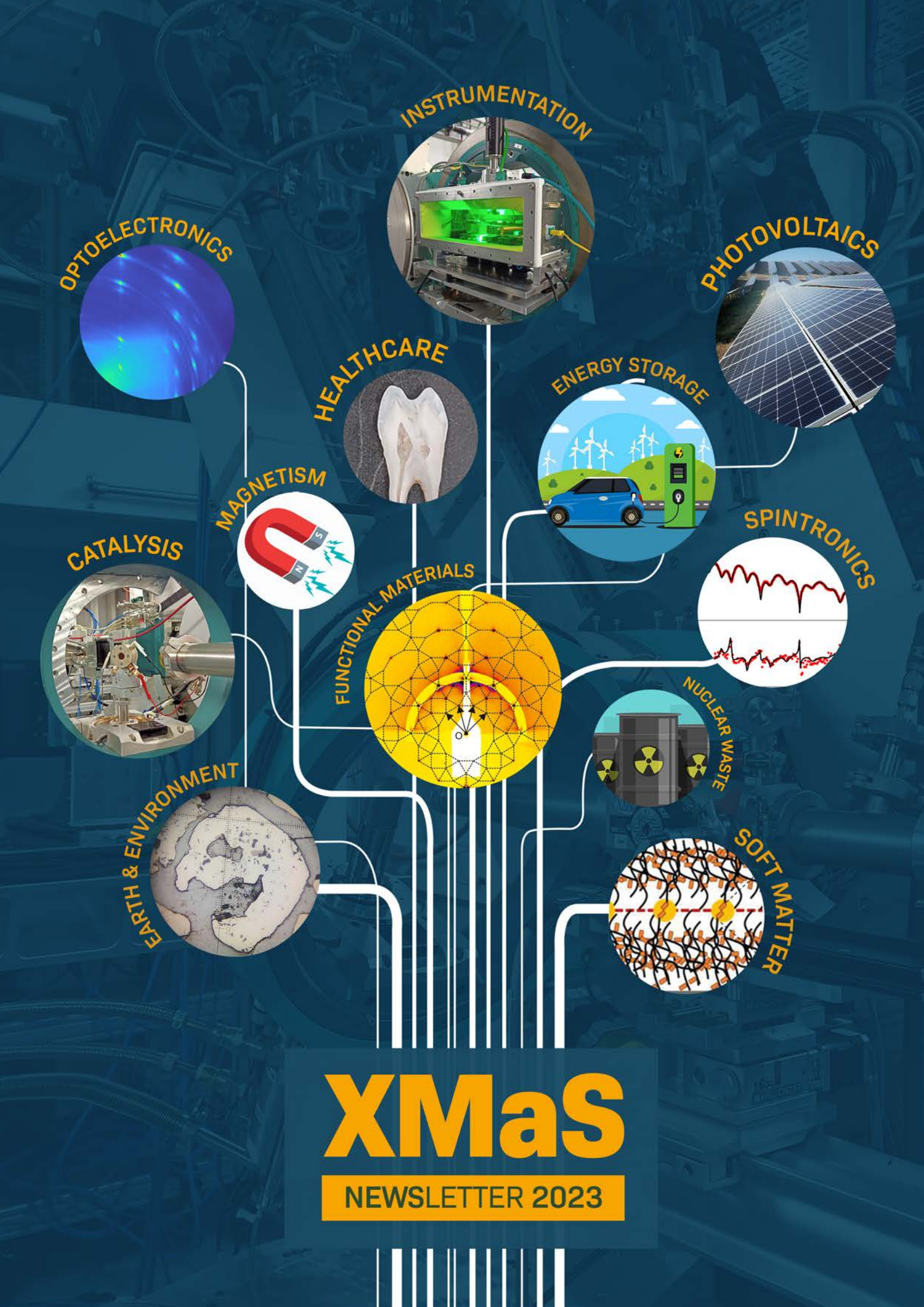

XMaS

NEWSLETTER 2023

CONTENTS

ON THE COVER:
XMaS encompasses a plethora of scientific areas and techniques, some of them being presented in the present Newsletter edition.

EPSRC funding until 2029!

It is with great pleasure that we can announce that EPSRC has approved funding for XMaS to continue until February 2029. The next 5 years will enable us to exploit the major upgrade of the facility, which took place during 2019/20, whilst the ESRF was undergoing the final part of the EBS upgrade. The new facility delivers a brighter X-ray beam with an extended operational range to higher photon energies thereby enabling new activities in materials research, particularly in terms of operando experiments. The new grant will extend the operating lifetime of the facility to over 30 years since operations first began in 1997. We would like to thank everybody in the User Community who responded promptly to the Statement of Community Need submitted in January 2023 and value your continuing support into the future.

It has been a busy year at XMaS with the first full year of normal user operation since the COVID pandemic. In May 2023 the beamline was evaluated by the ESRF SAC in its 5th quinquennial review. The report was very positive noting that *"the beamline is in excellent shape"*. Commenting on the uniqueness of the facility, it noted *"the new source has almost doubled the available energy range and allows users to swiftly change the incident energy range between tender and hard X-rays, which is very appealing for catalysis, energy and materials science."* The panel stated that *"the beamline's unique features can be exploited to allow combinatorial and multimodal analysis in many fields of material science. The staff are very competent, with complementary scientific background and can provide excellent support for the user community."* We thank the review panel for their very positive comments.

In addition to a full user programme a number of technical developments has been made in the last year. The KB mirror system was installed on the unfocused beam path in October 2023 by IDT Ltd with first commissioning in December 2023 yielding promising results (spot size 7 (V) µm x 5.5 (H) µm). Further commissioning will take place in 2024 before the system becomes available to users. New multi-element detectors, mainly for spectroscopy studies to exploit the new upper energy range of the beamline, have been delivered along with a new single element SDD to replace our old Vortex. Installation of all the detectors is planned during the first part of 2024. Other upgrades include the purchase of a Potentiostat/Galvanostat (to replace the 20-year old one) and a mass spectrometer for catalysis studies. A gas flow handling system is being designed in collaboration with the UK Catalysis Hub and this will allow rapid changes of the gas in the ionisation chambers and sample environments. Finally, a Raman spectrometer to allow simultaneous X-ray/Raman measurements was delivered at the end of 2023 although commissioning will be a relatively slow process due to the safety requirements for Class 3b lasers. If you are potentially interested in using this equipment please get in touch.

After 25 years under SPEC as our control system, we will gradually transition during the course of this year to BLISS, the new ESRF standard for hardware control and data collection. We will be advertising soon for a software engineer to help with this transition. On other staffing news in November 2023 our PDRA, Edgar Gutiérrez Fernández, left to take up a position within the software team at the ESRF. An advertisement for a new PDRA position to replace Edgar will be appearing soon at Warwick. We also lost our Warwick administrator, Sarah Jarratt, who moved to another role within the University. We wish both Edgar and Sarah all the best in their new positions and thank them for their wholehearted and invaluable contributions to the facility.

In terms of Outreach, the *XMaS Scientist Experience* (8th edition) took place in July 2023 with 16 competition winners visiting the ESRF and XMaS. Once again, we are indebted to the Synchrotron@School program [1] and the generosity of the ESRF in making this national competition the success it is and providing an opportunity to encourage young women into science. The next opportunity was launched in January 2024. We would appreciate any help in disseminating the trip and encouraging anyone who fits the brief to submit an entry [2].

Finally, in May 2023 it was a real pleasure to restart the XMaS Annual User Meetings with a meeting held in the Spine building at the University of Liverpool. Despite the best efforts of the national railway unions to disrupt this event by calling a one-day strike, over 50 people from across the UK and overseas attended the meeting and enjoyed an interesting day of talks and informal interaction whilst enjoying the spectacular views over the city and beyond. The next User Meeting will take place somewhere in the UK in the late spring/early summer.

Chris Lucas, Tom Hase, Yvonne Grunder and Malcolm Cooper

[1] https://www.esrf.fr/home/education/synchrotronschool.html
[2] www.xmas.ac.uk/impact/xmas_scientist_experienceb/

PyXscat

PyXscat is a new open-source software with a graphical user interface developed at XMaS/BM28 by our PostDoc Edgar Gutiérrez Fernández for both beginners and experienced users. It is used for quick visualisation and assessment of data quality during X-ray scattering/diffraction experiments. Focused on grazing-incidence geometry, it provides a limited but powerful toolkit, including integration methods, background subtraction, frame-averaging and grazing-incidence corrections. It is meant to be used during data acquisition and as a complementary tool for data reduction.

Its main assets are:
(a) Intuitive, fluid browsing of data files and metadata;
(b) Quick assessment of data quality and tuneable background subtraction;
(c) Automatic data reduction and visualisation;
(d) Implementation of grazing-incidence functionalities.

PyXscat is fully coded in Python and is built upon open-source code dependencies. The program reuses many existing and well-established packages and methods including some data handling packages developed at the ESRF (pyFAI, FabIO, pygix and silx toolkit). The code and the manual are publicly available at https://gitlab.esrf.fr/xmas-bm28/data_analysis/pyxscat.

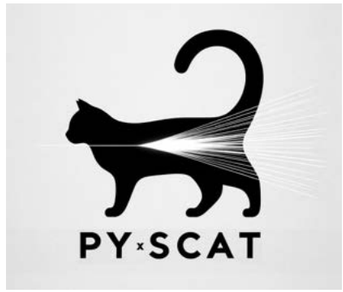

New GI-WAXS chamber for energy materials

One of the sources of performance instability in organic solar cells (OSCs) and photoactive devices is the light itself, what is called light soaking. To explore the structural effects triggered by the absorption of light in photovoltaic devices, a GI-WAXS chamber has been designed and fabricated to characterise high-efficiency OSCs under operando conditions (Fig. 1). Four samples can be mounted and illuminated with four different wavelengths or chromatic sections, corresponding to different regions of the solar emission spectrum (ultraviolet, white, green and near infrared). Their photovoltaic performance can be measured simultaneously through custom-made implemented electronics. Additionally, the chamber allows increasing the samples' temperature up to 100°C to perform accelerated aging experiments.

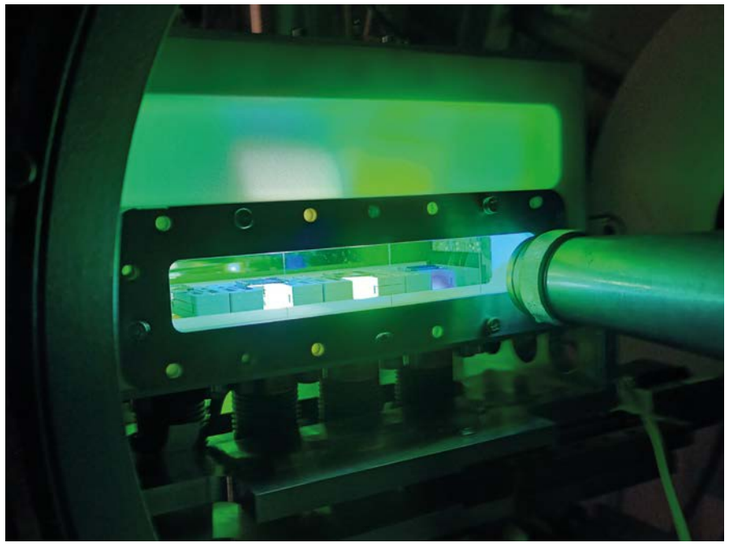

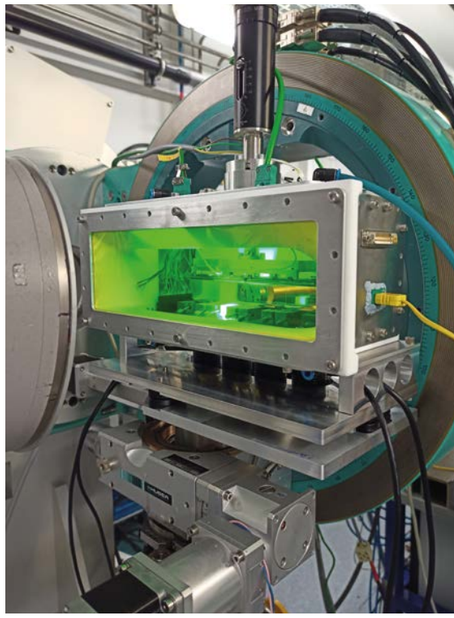

Fig. 1: New GI-WAXS chamber with an integrated sample support for simultaneous *in situ* and *operando* measurements of organic solar cells and photoactive devices under different illumination conditions.

Fast Energy Scanning

The ability to rapidly scan the energy across an absorption edge is crucial in spectroscopy when a chemical reaction may occur under the change of an external stimulus such as temperature, gas etc... Faster energy scans also increase the sample throughput and/or allow more experiments to take place. Good progress was made lately to implement this new capability. Hardware rewiring and macros within the control software (SPEC) were successfully implemented at XMaS allowing preliminary tests to be carried out in transmission XAS using ion chambers as monitor and detector (Fig. 2). The so-called *zapscans* are fully consistent over the EXAFS energy range with the step-by-step approach used before (*Escan*). For comparison at the Ag K-edge, the *Escan* took 8 min whilst the *zapscan* took 15 s. The implementation is yet to be tested in fluorescence XAS at different energies using the energy dispersive (SDD and Ge) detectors and for different sample concentrations in order to determine the lower limits above which *zapscan* can be utilised.

Fast multi-motor scans will also be possible in the future when the new ESRF standard control system, BLISS will be implemented. The migration from SPEC to BLISS will begin in 2024.

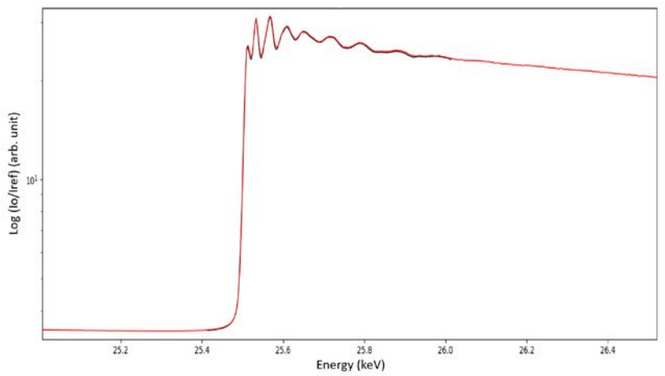

Fig. 2: Comparison between EXAFS data recorded using the conventional step scan (0.2 s/pt, black) and the fast scanning (50 ms/pt, red) at the Ag K-edge. The XANES part was collected in 15 s in *zapscan* mode and in 8 min with the standard *Escan* (step scan).

KB mirror system

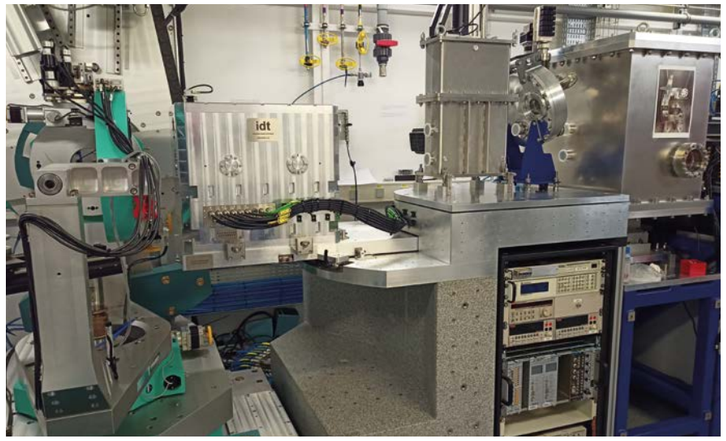

Fig. 3: The IDT KB mirror system sitting in the monochromatic unfocused beam (MUB) path. The granite table is shaped to allow the rotation of the nu circle (horizontal 2θ) counterweight. The system is fully retractable to a park position by means of a circular rail track.

The new KB mirror system was installed by IDT Ltd [1] in early autumn 2023 (Fig. 3). The custom design ensures operation between 4 and 25 keV (Pt, Rh stripes and bare Si).

The system is housed on the unfocused beam (MUB) path and does not impede normal focused beam (MFB) operations as this beam passes uninterrupted through the vessel assembly. The design of the system also allows it to move out of the beam on a rotation to revert back to a more standard MFB configuration when more space is needed (see *2021 XMaS Newsletter*). The reproducibility of the movement is still to be determined but preliminary trails indicate that the KB focused beam remains at the same place when the focused KB assembly is switched.

A spot size of ~5.5 (H) x 7 (V) μm² has already been measured in the first commissioning round in December 2023. More development is needed to make the whole focusing system more user-friendly, notably on the monitor/detector part. User availability is expected towards the end of the year.

[1] IDT Ltd (www.idtnet.co.uk)

Resonant X-ray study of spatial magnetisation mapping in ferrimagnetic rare-earth: transition-metal alloy thin films for spintronics

O. Inyang, D. Rianto, C. Swindells, L. Bouchenoire, R.J.H. Morris, A. Merkulov, A. Caruana, C. Kinane, T.P.A Hase, D. Atkinson

Rare-earth (RE): transitional metal (TM) alloys have been a recent focus of significant spintronics research. However, recent evidence shows that within a given RE:TM thin film, the distribution of constituent atomic species appears non-uniform. This has been attributed to the segregation of RE atoms at the surface [1] or the coexistence of separate crystal phase clusters [2], which may result in non-trivial magnetic responses [3].

In our study, we explored the elemental distribution and magnetisation profiles across the thickness of nominally uniform $Gd_{23}(Co_{10}Fe_{90})_{77}$ sputtered thin films. X-ray Resonant Magnetic Reflectivity (XRMR) was measured at the Gd L_3-edge on XMaS/BM28, providing insights into both depth-dependent structural and the element-specific magnetic profile of Gd. Fig. 4(a) and 4(b) present specular reflectivity and magnetic asymmetry data respectively, along with the best-fitted simulation of the XRMR data obtained using GenX. Fig. 4(c) illustrates the spatial distribution of the electron density (black line) within the GdCoFe layer, while the magnetic Scattering Length Density (SLD) profile (red line) acts as a proxy for the Gd moment, exhibiting a peak at the central layer.

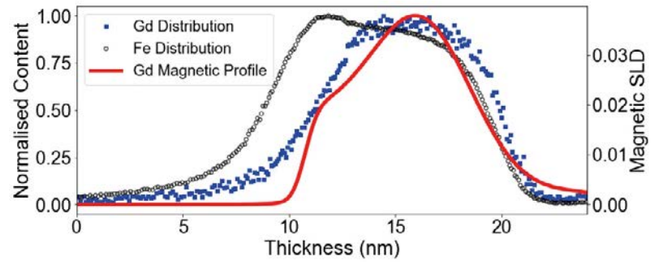

Fig. 5: Fe and Gd compositional profiles plotted with the Gd magnetic SLD within the GdCoFe layer. Note that the Gd moment distribution does not simply follow the Gd elemental distribution, suggesting the Gd moment is sensitive to the local compositional environment.

Compositional mapping via Secondary electron Ion Mass Spectroscopy (SIMS) is plotted alongside the Gd magnetisation profile in Fig. 5, demonstrating that the Gd moment aligns with the Gd distribution, peaking at the central layer. However, complexities arise near the interfaces, where the Gd moment is enhanced close to the Pt interface, correlating with a peak in Fe content. No such enhancement occurs at the W interface. These findings suggest that compositional variations alter the local electronic environment of Gd.

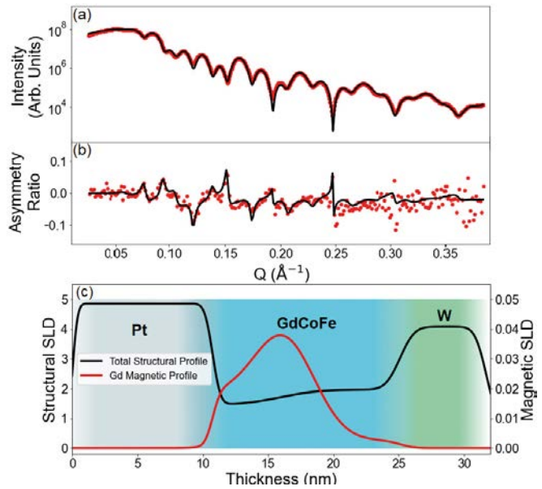

Fig. 4: (a) Specular reflectivity and (b) spin asymmetry data measured at Gd L_3-edge. The black lines are the best fitting simulations. (c) Structural and magnetic SLD profiles in the Pt/GdCoFe/W structure extracted from the simulation.

Our results showcase the capabilities of XRMR in exploring depth-dependent magnetisation behaviour in spintronic heterostructures [4]. When combined with SIMS, these techniques reveal complex spatial variations dependent on elemental species. These findings have significant implications, as non-uniformities directly impact spin transport properties, playing a key role in advancing future spintronic device technologies based on RE:TM alloys.

[1] N. Bergeard *et al.*, Phys. Rev. B 96, 064418 (2017).
[2] V.G. Kudin *et al.*, Semicond. Phys. Quantum Electron. Optoelectron. 24(1), 56 (2021).
[3] A. Chanda *et al.*, Phys. Rev. B 104, 094404 (2021).
[4] O. Inyang *et al.*, Appl. Phys. Lett. 123, 122403 (2023).

For more information, contact
D. Atkinson,
Department of Physics,
University of Durham, UK.
del.atkinson@durham.ac.uk

New molecules for evaporated organic solar cells

P. Kaienburg, I. Habib, O. Gough, M. Riede

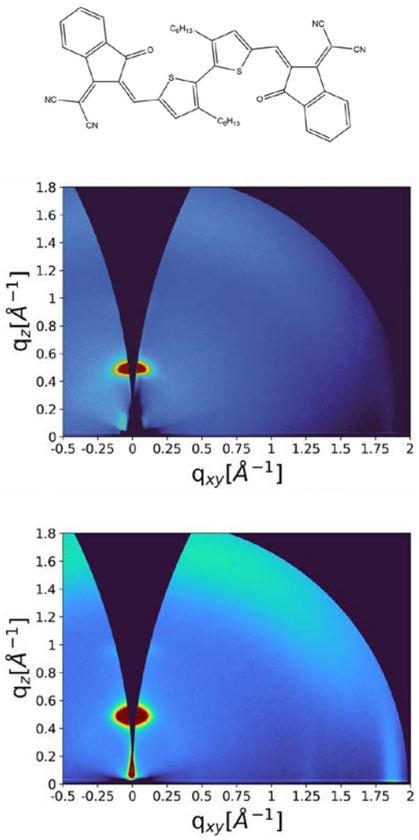

Fig. 6: Molecule structure of BTIC-H NFA (top). GI-WAXS data of films deposited at room temperature (middle) and on an 80°C heated substrate (bottom). The heated deposition shows a higher degree of order.

Organic solar cells (OSC) offer unique features for harvesting solar energy [1]: they weigh less than conventional silicon solar panels and can be made flexible. They can also be fabricated in semi-transparent and color-selective designs – making them appealing to architects and for integration into greenhouses.

Such solar cells can be made either wet-chemically from solution or through thermal evaporation in vacuum. The latter route is leading in industry, which already applies it for manufacturing OLED displays in smartphones and TVs [2]. However, due to the ease of sample preparation, academic research has embraced solution processing and developed an impressive range of high-performing molecules. So-called *non-fullerene acceptors* (NFAs) are at the heart of the latest improvements. The Oxford-based team is researching how to transfer high-performing materials to industrially relevant vacuum deposition.

In collaboration with Prof. Weiwei Li's Beijing-based group, such candidate molecule named BTIC-H (see Fig. 6 top) was synthesised and tested [3]. This entailed optoelectronic characterisation of the absorption coefficient, thin-film energy levels and charge carrier mobility. The molecule was then paired with a range of electron-donating partners and made into devices, i.e. functional solar cells.

From determining the power conversion efficiency alongside other key performance characteristics and an in-depth energy loss analysis, the BTIC-H performed similar but slightly worse than the incumbent C_{60} acceptor molecule. PI Prof. Moritz Riede reported that *"The initial results are very encouraging but not quite yet the breakthrough we need but we do see a clear path forward!"*

This is also the first report of a standard protocol that the team has developed for efficiently screening new molecules. For example, one practical advantage of evaporating organic semiconductors is the ability to form planar heterojunctions, which allow disentangling interface energetics from the mixing behaviour of molecules.

The team believes that the way these organic semiconducting molecules pack, stack and aggregate plays a critical role in delivering all the advantages that this class of molecules has demonstrated. Getting an in-depth understanding of the arrangement of the molecules is thus vital to understand why a specific molecule works or does not work well. The microstructure of the non-fullerene acceptor BTIC-H was investigated on XMaS/BM28 using Grazing-Incidence Wide Angle X-ray Scattering (GI-WAXS).

The GI-WAXS data clearly showed that the packing of the BTIC-H molecule can be tuned by heating the substrate during deposition (see middle and bottom panel of Fig. 6). The results [3] are a starting point for future work on NFAs in our group in pursuit of a small revolution on how we produce solar energy.

[1] P. Kaienburg *et al.*, *"Roadmap on Photovoltaic Materials for Sustainable Energy Conversion"– Organic PV* (ch. 6), https://arxiv.org/abs/2310.19430.
[2] M. Riede *et al.*, Adv. Energy Mater. 11, 2002653 (2021).
[3] I. Habib *et al.*, APL Mater. 11, 061128 (2023).

For more information, contact

P. Kaienburg,
Department of Physics,
University of Oxford, UK.

Pascal.kaienburg@physics.ox.ac.uk

Structural study of organic thin films for optoelectronic devices with Grazing-Incidence Wide Angle X-ray Scattering

C. Fynbo, Mathias K. Huss-Hansen, O. Bikondoa, C. Gangadharappa, D.A.D.S. Filho, S. Patil, M. Knaapila, and J. Kjelstrup-Hansen

Organic semiconductors (OSC) are widely used in organic optoelectronics due to their high optical absorption and structural versatility compared to their inorganic counterparts. Besides the intrinsic properties of the OSC material, device performance is mainly determined by the morphology and crystalline structure of the organic film and the material interfaces in the device. Due to the anisotropic shape of most OSC molecules, the molecular packing and therefore the charge and energy transport in the film will be anisotropic in nature as well [1].

We have combined Grazing-Incidence Wide Angle X-ray Scattering (GI-WAXS) with specular X-ray Diffraction (XRD) and Atomic Force Microscopy (AFM) to investigate the crystalline structure and morphology of thin films made from a diketopyrrolopyrrole derivative OSC [2]. GI-WAXS uses a small angle between the incoming X-ray beam and the sample making it possible to probe only the thin film without contribution from the substrate. The intensity and position of the scattering peaks reveal information about the degree of crystallinity and molecular packing of the thin film.

Spin-coated OSC films show a fiber-like morphology (final form) (Fig. 7d) and pronounced structural order in both in-plane and out-of-plane directions (Fig. 7a). Initially, the spin-coated films revealed the presence of two distinct morphologies and crystalline phases immediately after fabrication. However, the initial metastable phase evolved into the more stable crystalline phase after a couple of days, coinciding with the transformation from a continuous film to a film morphology consisting of fibers (Fig. 7b-e). The stable phase has been shown to exhibit higher charge carrier mobility [3].

These results strongly suggest that GI-WAXS and specular XRD are useful tools in understanding the microstructure and its evolution in OSC thin films, and can thereby support development of organic optoelectronic devices.

[1] T. Breuer *et al.*, ACS Appl. Mater. Interfaces 9, 8384 (2017).
[2] C. Fynbo *et al.*, Langmuir 39, 34, 12099 (2023).
[3] A. Pickett *et al.*, ACS Appl. Mater. Interfaces 10, 19844 (2018).

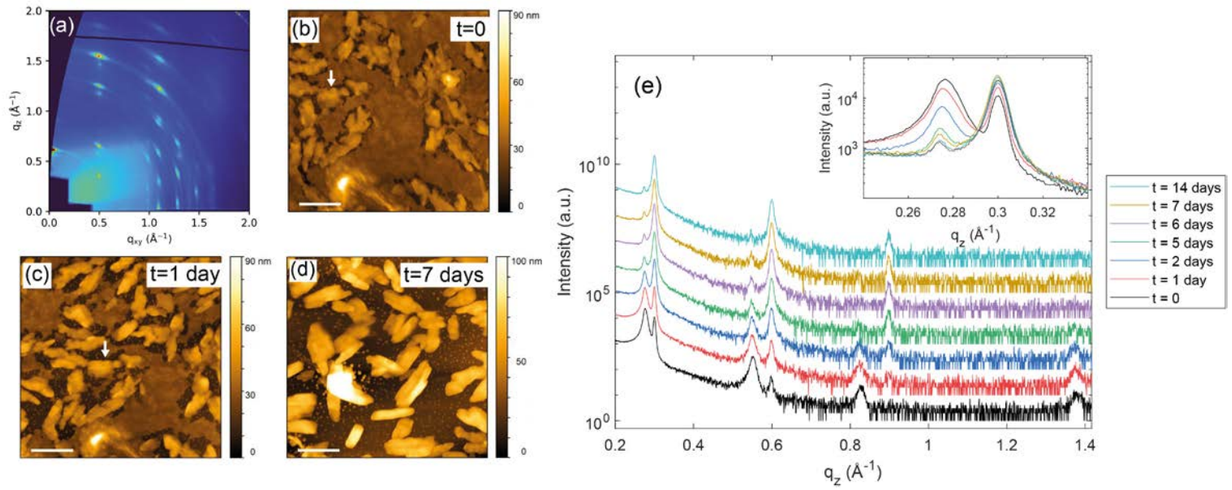

Fig. 7: Spin-coated OSC film. (a) 2D GI-WAXS pattern collected on XMaS/BM28. (b), (c), and (d) AFM images taken at different time intervals after spin-coating. The scale bar is 2 µm. The white arrows point to the same structure in (b) and (c) but are not visible in (d) due to thermal drift of the AFM setup. (e) Specular XRD curves measured at different time intervals after spin-coating. The curves are offset for clarity. Insert: same curves plotted in the region q_z = 0.24-0.34 Å^{-1}.

For more information, contact

C. Fynbo, NanoSYD,
Mads Clausen Institute,
University of Southern Denmark, Denmark.

cfynbo@mci.sdu.dk

A different story of AI: Amelogenesis Imperfecta

A. Harfoush, M. Al-Mosawi, R.P. Davies, N. Thomson, M. Al-Jawad

Amelogenesis Imperfecta (AI) is a genetic disorder that affects the enamel formation on teeth. Enamel is the outermost layer of your teeth. It is tough, protective and acts as a bodyguard that keeps your dentition safe from cavities and decay. Enamel of people suffering from AI is often thin, discoloured and prone to wear and tear (Fig. 8). More importantly, AI can lead to lower self-esteem, social stigma and potential bullying arising from visible dental abnormalities. Individuals may face body image concerns, emotional stress and treatment-related anxiety, affecting overall well-being [1]. Current treatment involves a lifetime of chairside care at significant cost to health care providers.

Fig. 8: Clinical images demonstrating the manifestations of AI. Teeth are usually yellowish to brownish in color, pitted or/ and decayed.

To understand how AI develops, our University of Leeds research team used X-Ray Diffraction (XRD) on XMaS/BM28. We analysed teeth extracted from AI-diagnosed patients to identify key pathways in hard tissue formation. AI teeth were collected from the School of Dentistry Skeletal Tissues Bank (REC 13/YH/0028), University of Leeds. First, these samples were scanned intact using a micro-computed tomography machine in order to identify the mineral density changes. They were then sectioned into 200 µm thick slices for the synchrotron XRD in order to map the texture and organisation of enamel crystallites [2]. The microstructural and compositional changes were determined using Scanning Electron Microscopy (SEM) and Energy-Dispersive X-ray spectroscopy (EDX).

The XRD data (Fig. 9) reveal that the crystallite organisation of enamel [3] is influenced by the disease at the nano-scale level, especially near inner enamel and cuspal areas. This suggests that AI likely resulted in the retention of more proteins within the enamel during development hindering crystal growth. This phenomenon may explain the compromised mechanical properties and the rapid breakdown of enamel shortly after eruption.

The observation of greater impact on the inner enamel and cuspal areas implies that the gene responsible for AI in this case acted during the early stages of enamel formation, specifically during the secretion/ maturation phase. As enamel typically originates from the inside and spreads outward, the higher susceptibility of the inner enamel suggests an early-stage influence of the AI-causing gene. Thus, this highlights a more crucial timeframe for the action of the MMP20 gene during the process of enamel formation.

[1] C.E.L. Smith *et al.*, Front. Physiol. 8, 435 (2017).
[2] A. Al-Jawad *et al.*, Key Eng. Mater. 361, 877 (2008).
[3] A. Harfoush *et al.*, expt. XMaS/BM28, A28-1-1339.

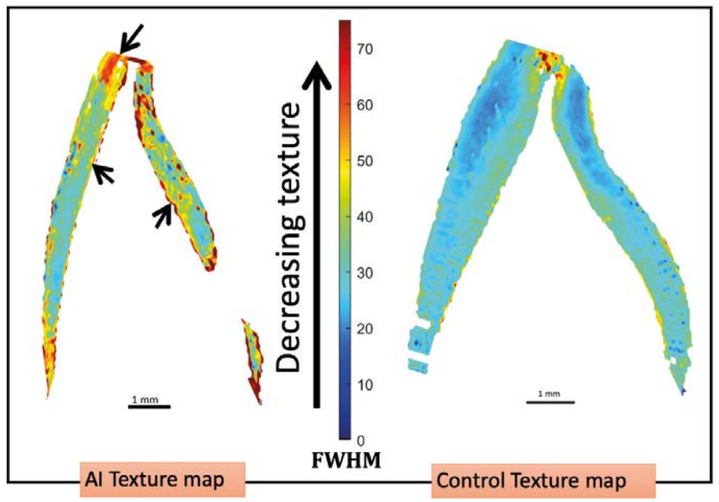

Fig. 9: XRD results of an AI-affected tooth slice (left) and its matching control (right). Note the disorganised nature of the enamel's crystallites at the cusp and inner enamel (arrows – yellowish to reddish range), whereas the control tooth shows healthy crystallite organisation as the map shows lower values for FWHM indicted by the bluish to greenish range.

For more information, contact

A. Harfoush,
Department of Oral Biology,
University of Leeds, UK.

dnaah@leeds.ac.uk

"*Centipede*" statistical polymer under nano-confinement

N.M. Taylor, O. Bikondoa, P.J. Dowding, B. Vincent, W.H. Briscoe

Controlling friction and wear between contacting surfaces in relative motion is important to sustainability in a wide range of industrial and engineering scenarios, with immense economic, environmental, and societal impact. An estimated 20% of the world's energy consumption (equivalent to 103 EJ) is spent overcoming friction within tribological contacts. The development of new lubrication strategies is therefore crucial to reducing friction and wear, improving energy efficiency, and reducing global emissions of CO_2 and other pollutants. It is also relevant to efficient and safe operation in future transportation (e.g. electrical vehicles) and off-shore energy generation (e.g. wind turbine bearings).

In this context, polymers have been widely used as additives to mediate surface forces and friction. Such interactions depend sensitively on the polymer conformation at the interface (e.g. end-anchored brushes, surface aggregates, or loops and trails), which in turn depends intimately on the polymer molecular architecture.

Here we report surprising interfacial behaviour, through direct measurement of surface forces and friction mediated by a functionalised statistical copolymer in n-dodecane using the Surface Force Apparatus (SFA) [1]. The bespoke-architecture polymer has an olefin backbone decorated with a statistical distribution of polar-aromatic functional side-groups, with a structure that we term as *"centipede"* (Fig.10a inset). The polymer is anchored on the mica surface in SFA through either physisorption or using the classic Langmuir-Blodgett (LB) method, i.e. transferred from the air-water interface of an LB trough with the polymer nanofilm thickness and density controlled via the transfer surface pressure Π.

As the LB-polymer layers are brought into nano-confinement in the SFA, the surface forces (F_n) observed can be described by the classic Alexander-de Gennes theory (solids lines, Fig.10a), with the onset surface separation for the surface force far exceeding the thickness of an LB-polymer-monolayer. This is confirmed by complementary synchrotron X-Ray Reflectivity (XRR) measurements at XMaS/ BM28, indicating a multilayer structure. Compared to adsorbed polymer layers, the LB polymer layers can mediate *superlubricity* (with a friction coefficient as low as 0.0002, comparable to that found in human articular joints).

Based on the SFA and XRR results, we propose that molecular arrangement upon LB compression leads to the multilayer nanofilm with a structure akin to an interfacial gel, with the transient crosslinking facilitated by the intra- and inter-molecular interactions between the functional groups (Fig.10b). These results also point to the potential route to tailor the polymer architecture, e.g. the nature, density, and distribution of the functional groups, for controlling the interfacial structure and the nanotribological properties of confined macromolecular layers.

[1] N.M. Taylor *et al.*, J. Colloid Interface Sci. 653, 1432 (2024).

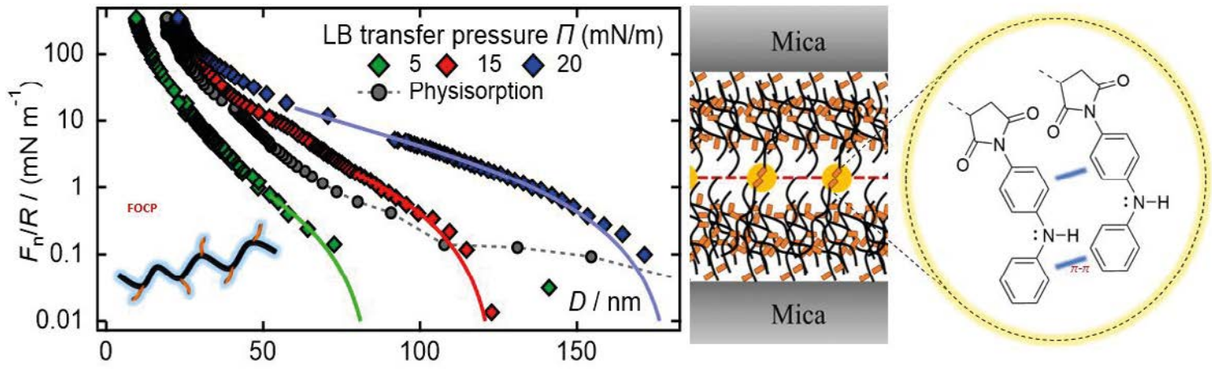

Fig. 10: a) SFA results with the "centipede" polymer structure shown in inset; b) Proposed interfacial gel structure mediated by sticky groups.

For more information, contact

W. Briscoe,
School of Chemistry,
University of Bristol, UK.

wuge.briscoe@bristol.ac.uk

2D Quasicrystal from self-assembled polygonal nanocolumns

X.B. Zeng, B. Glettner, Ute Baumeister, Bin Chen, Goran Ungar, Feng Liu, C. Tschierske

The discovery of quasicrystals in metal alloys in 1984 **[1]** - a Nobel prize winning work - changed our preconception that any structure with long-range positional order must be periodic. While a common crystal can be described as a periodic repetition of a single unit cell, a quasicrystal has multiple building blocks (tiles) of different shapes, with a symmetry such as pentagonal or dodecahedral that is incompatible with a periodic lattice. To keep the long-range positional order without periodicity, strict and often complex tiling rules must be followed.

The first liquid quasicrystal (LQC) was discovered in 2004 **[2]**. Since then more nano- and meso-scale quasicrystals were found in other soft and hard synthetic systems. The unusual combination of long-range positional order and high rotational symmetry makes nanoscale quasicrystals interesting for applications e.g. in wide band-gap photonics. However, we are still very limited in our ability to control the formation of nano-tiles of different shapes through self-assembly, and to guide the packing of such nano-tiles into quasiperiodic structures through their intricate interactions.

Zeng *at al.* reported the discovery of the first columnar liquid quasicrystal (CLQC) **[3]**. The unusual symmetry of the CLQC is demonstrated by the 12-fold rotational symmetry of its Grazing-Incidence X-Ray Diffraction (GI-XRD) pattern (Fig. 11-centre, recorded at XMaS/BM28) from a surface-oriented thin film, equivalent to that from a single CLQC crystal rotating around its vertical axis. The dodecagonal reciprocal lattice, overlaid on the GI-XRD pattern, clearly shows the 12-fold rotational symmetry and the coincidence of experimental spots and the theoretical lattice nodes.

The compound studied is a T-shaped molecule, consisting of a rigid rod-like aromatic (p-terphenyl) core, two alkyl end-chains and a polar ionic group attached to an oligo-ethylene oxide lateral chain (Fig. 11, top left). Due to the tendency of the three incompatible but connected parts to nanophase separate, such T-shaped polyphiles are extremely versatile in forming different 1D, 2D and 3D liquid crystal (LC) structures. These include the "honeycomb" type, consisting of columns with a range of polygonal cross-sections **[4]**. The rigid molecular cores form the flat sidewalls of the prismatic columns, their end-groups aggregating at column edges and the lateral chains occupying the interior.

The CLQC structure has been determined to consist of triangular, square and trapezoidal columns. A dodecagon, consisting of four triangles, one square and two octagons, is the basic tile that has been used to generate the unique dodecagonal quasi-periodic tiling of the plane (Fig. 11, top right). It was also shown that the driving force for quasiperiodicity in this new CLQC could be attributed primarily to optimisation of packing, i.e. lowering of the system energy rather than increasing the randomness-entropy as in the case of previously found soft quasicrystals.

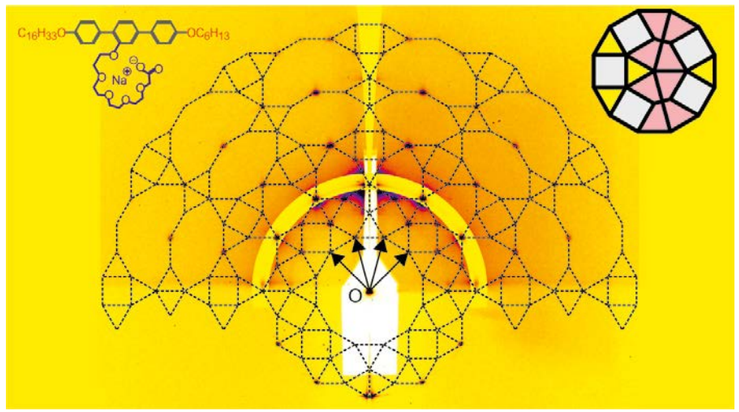

Fig. 11: GI-XRD pattern of CLQC showing 12-fold symmetry (centre). T-shaped Molecule (top left). Dodecagonal tile formed by triangular, square and trapezoidal columns (top right).

[1] D. Shechtman, Phys. Rev. Lett. 53, 1951 (1984).
[2] X.B. Zeng *et al.*, Nature 428, 157 (2004).
[3] X.B. Zeng *et al.*, Nat. Chem. 15, 625 (2023).
[4] X.B. Zeng *et al.*, Science 331, 1302 (2011).

For more information, contact

X.B. Zeng,
Department of Materials Science and Engineering,
University of Sheffield, UK.

x.zeng@sheffield.ac.uk

Sugar alternatives for processing radioactive waste

J.C. Rigby, D.R. Dixon, J. Kloužek, R. Pokorný, P.B.J. Thompson, A. Scrimshire, A.A. Kruger, A.M.T. Bell, P.A. Bingham

The coming year will see operations commence at the Hanford Waste Treatment and Immobilization Plant (WTP) in Washington State, USA. The Hanford site has historically stored radioactive waste generated from 1944 through to 1989 in 177 carbon-steel tanks in shallow repositories. The quantity of waste and chemical variability between the tanks amount to the country's most complex clean-up effort, regularly faced with unique challenges **[1]**.

For high-level waste (HLW) waste slurry will be mixed with glass-forming chemicals and fed into the top of a Joule-Heated Ceramic Melter, shown in Fig. 12, and heated to 1150°C. The final product is a melt that will exit through the glass-discharge port and into a steel cannister where it will cool to form glass. This glass will keep the radioactive isotopes it contains stable and isolated for over a thousand of years **[2]**.

During the process of melting, gases evolving can become trapped in foam within the layer of reacting melter feed, the cold cap (Fig. 12), which can reduce the glass production rate by decreasing the heat transfer. To combat this, sugar (sucrose) is added to manage foaming via controlling the feed and melt redox state. However, in certain cases, sucrose addition produces further toxic and undesirable gases.

In simulated feeds, formic acid, hydroxyethylenediaminetri-acetic acid (HEDTA), coke dust and graphite were evaluated as alternatives to sucrose. Results show the foam volume reduction correlates with carbon content of the reductant; coke dust (93% C) and graphite (99+% C) outperformed sucrose, formic acid and HEDTA **[3]**.

A decrease in foam volume alone is insufficient for successful melter processing. A full understanding of the effects on the oxidation state of key multivalent species in the system during melting, and particularly the final glass, evaluates likelihoods of precipitation of metallic species, sulphides or excessive crystalline phases detrimental to both the melter system and the integrity of the glass for long-term radioisotope immobilisation.

Investigation of the redox behaviour of the multivalent elements Fe, Cr, Mn, Ni and Ce with temperature and reductant addition was undertaken at XMaS/BM28 using X-ray Absorption Near-Edge Spectroscopy (XANES) in simultaneous fluorescence and transmission modes. The XANES spectra were collected at the K-edges of Fe, Cr, Mn, Ni and at the L_3-edge of Ce.

This element specific technique allowed for clarity of examination of the structure of these species despite the complex chemical matrix. Fig. 13 is an example of the % reduced species in the graphite containing feed. This also gave a coherent understanding of the oxygen balance in the melt at different temperatures, which effects the foam behaviour **[3]**.

The work performed enabled assessment of alternate reductants to sucrose in HLW feeds that could improve operating efficiency, flexibility and compositional variability.

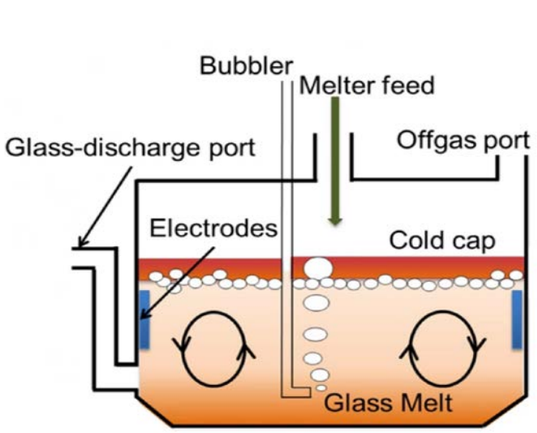

Fig. 12: Schematic of a Joule-Heated Ceramic Melter designed to vitrify HLW.

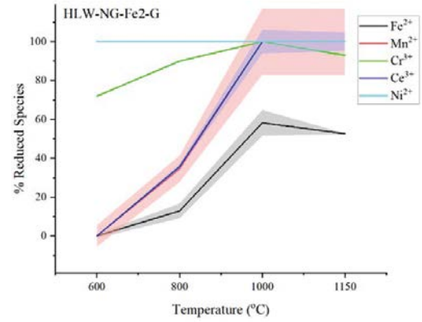

Fig. 13: % of reduced species of Fe, Mn, Cr, Ce and Ni with temperature using graphite as a reductant [3].

[1] J. Marcial *et al.*, J. Hazard. Mater. 46, 1324371 (2024).
[2] C.L. Thorpe *et al.*, NPJ Mater Degrad. 5, 61 (2021).
[3] J.C. Rigby *et al.*, J. Non-Cryst. Solids, 608, 122240 (2023).

For more information, contact

J.C. Rigby,
Pacific Northwest National Laboratory,
Richland, WA, USA.

jessica.rigby@pnnl.gov

Transforming bio-diesel waste into green hydrogen and chemicals

H. Luo, V. Y. Yukuhiro, P. S. Fernández, J. Feng, P.B.J. Thompson, R.R. Rao, R. Cai, S. Favero, S.J. Haigh, J.R. Durrant, I.E. L. Stephens, M.M. Titirici,

Bio-diesel by-product glycerol electro-oxidation reaction (GEOR) to co-produce green H_2 and valuable chemicals at low potential constitutes a promising strategy to phase out fossil fuels in the energy and chemical sectors [1]. PtNi bimetallic electrocatalysts are promising candidates for GEOR. However, the role of Ni remains unknown.

The work lead by H. Luo and R. Rao from Imperial College London, aimed to investigate the role of Ni in PtNi electrocatalysts. Using X-ray absorption spectroscopy (XAS) at XMaS/BM28, we were able to examine the local atomistic and electronic structure of Pt and Ni and construct a precise model for a series of PtNi bimetallic nanoparticles (Fig. 14). The X-ray Absorption Near Edge Structure (XANES) spectra collected at the Pt L_3- and Ni K-edges showed that both Pt and Ni are partially oxidised. From the Extended X-ray Absorption Fine Structure (EXAFS), the Pt–Pt pair coordination number follows a descending trend from PtNi1 to PtNi3, indicating less Pt rich local areas. The results also show that the Pt–Ni pair coordination peak is the highest for PtNi2 suggesting that the atoms are most homogeneously coordinated, consistent with the Scanning Transmission Electron Microscopy (STEM) results.

PtNi2 exhibits the highest GEOR activity normalised to the mass and surface area. From examining the partial current density towards glycolate (through C-C bond cleavage), we propose that higher Ni content in PtNi can also significantly promote the partial C-C bond cleavage towards glycolate formation. These results demonstrate that Ni plays a significant role in PtNi's performance towards GEOR.

With further work combining *operando* XANES with online UV-Vis spectroscopy, we schematically illustrate the role of Ni in PtNi catalysts for GEOR: the surface Ni atoms form $Ni(OH)_x$ islands in alkaline conditions and get poisoned by glycerol molecules, blocking the sites for *OH adsorption, and thus do not participate in the overall reaction. Instead, the presence of Ni modulates the electronic structure of the surface Pt atoms, weakening the *CO and *OH binding energy. The Pt–Ni structure in PtNi2 induces the most optimised *CO and *OH adsorption strength on Pt sites, thereby displaying the highest activity in this study. Such fundamental insight into the GEOR paves the way for the design of catalysts with selective electrochemical alcohol oxidation.

[1] H. Luo *et al.*, Adv. Energy. Mater. 11, 2101180 (2021).

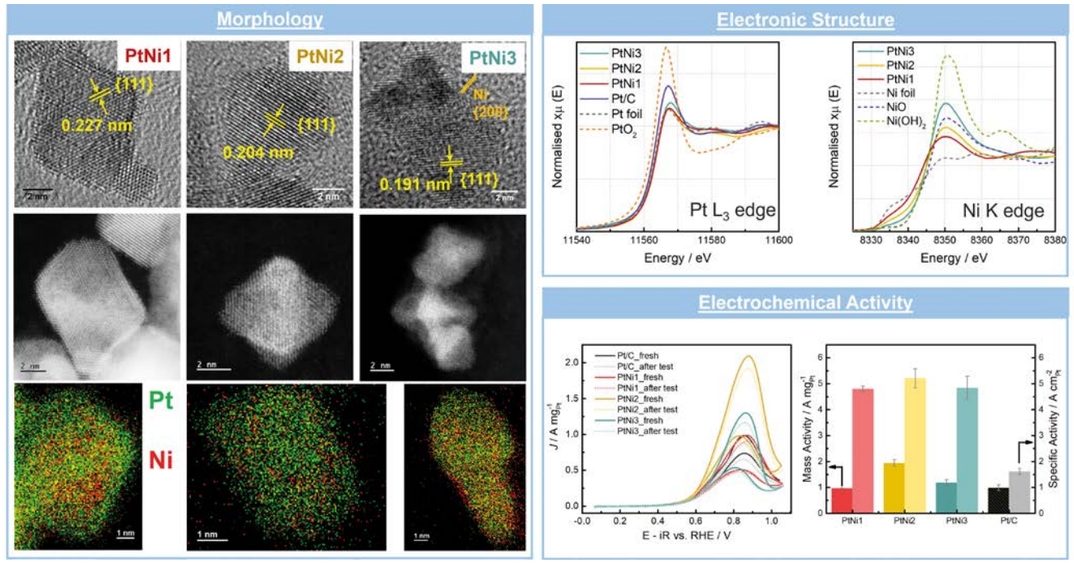

Fig. 14 **Morphology**: TEM, atomic-resolution aberration-corrected HAADF-STEM images and EDX mapping of PtNi catalysts; **Electronic Structure:** Pt L_3- and Ni K-edges XANES spectra of three as-prepared PtNi samples, ex-situ, compared with reference materials; **Electrochemical Activity**: (left): cyclic voltammetry profiles of all catalysts before/after test; (right): the corresponding mass and specific activities.

For more information, contact

H. Luo,
School of Mechanical Engineering Sciences,
University of Surrey, Guildford, UK.

hui_luo@surrey.ac.uk

Observing the incorporation of small heteroatoms into palladium metal

L.G. Costley-Wood, K. Mohammed, M. Carravetta, D. Decarolis, A. Goguet, A. Kordatos, R. Vakili, H. Manyar, E. McPake, C. Skylaris, P.B.J. Thompson, E. Gibson, P.P. Wells

The element palladium (Pd) plays a huge role in industrial scale chemical processes. It is employed as a catalyst, a species that improves the efficiency of the reaction, providing an alternative pathway. Examples of such chemical processes are the transformation of pollutant exhaust emissions such as CO and NO_x in petrol vehicles, and the crucial removal of impurities during polyethylene (plastic, PET) formation.

Pd's impressive ability to control and improve these reactions is partly down to the incorporation of heteroatoms into its metal structure during reaction [1]. These are atoms of elements including carbon, hydrogen and nitrogen, present in the reaction mixture, which migrate into the Pd particles and sit in an "interstitial" position. They can be consumed and then replenished during reaction.

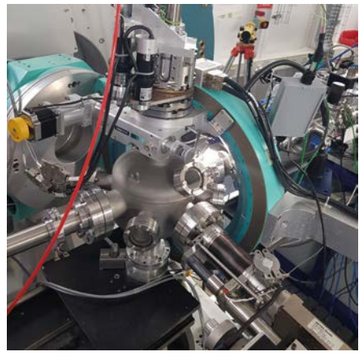

Fig. 15: Sample ready for X-rays in a helium chamber at XMaS.

Impressive amounts of research have been performed on the carbon (PdC) and hydrogen (PdH) structures, but nitrogen (PdN) is much newer to the party. The first experiments which observed PdN formation and postulated its role in certain chemical reactions were performed only in the last few years [2,3].

Our research collaborative work between the Universities of Southampton, Glasgow and Belfast, took place on XMaS/BM28 (Fig. 15) using X-ray Absorption Near Edge Spectroscopy (XANES). The aim was to observe PdC, PdH and PdN formation on one catalyst, and test their stability under different conditions. This was coupled with computational analysis on the PdN, providing additional information to couple with the experimental results. The tender X-rays available at XMaS were essential here, being more sensitive to such small changes to the Pd metal structure.

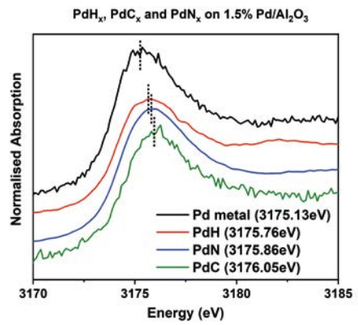

Fig. 16: The difference in absorption edge position of Pd structures at the Pd L_3-edge.

Fig. 16 shows the XANES spectra collected across the Pd L_3-edge for the different Pd structures formed during the experiment. The position of the first peak is different for the different heteroatoms; this is partly related to their different sizes. The observed stabilities of the PdC and PdN are described by Fig. 17. Under hydrogen, PdN immediately decomposed back to something resembling pure Pd metal. The PdC was stable a while longer, but signs of decomposition were observed from 140°C. Under helium, the PdC remained stable to the highest tested temperature of 220°C, though literature suggests this extends to above 600°C. The PdN was stable only to 120°C.

The experiment succeeded in forming all three structures on one catalyst for the first time [4]. The knowledge gained potentially paved the way for further tuning the performance of Pd catalysts, which form PdN structures during reaction.

[1] T. Xie *et al.*, Catal. Today 371, 29 (2021).
[2] E. K. Dann *et al.*, Nat. Catal. 2, 157 (2019).
[3] D. Decarolis *et al.*, ACS Catal. 11, 2141 (2021).
[4] L.G. Costley-Wood *et al.*, ChemCatChem 15, e2023008, 9 pp (2023).

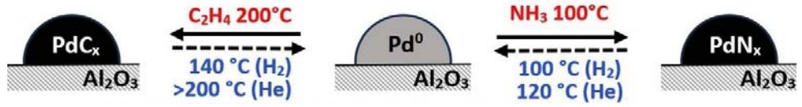

Fig. 17: The formation and decomposition conditions of PdN and PdC.

For more information, contact

P.P. Wells,
Department of Chemistry,
University of Southampton, UK

p.p.wells@soton.ac.uk

Speciation and characterisation of Se in Pt-Pd-substituted pyrite

O.N. Filimonova, O. Bikondoa, L. Bouchenoire, P.B.J. Thompson, D. Wermeille

The rapid rise in demand for "critical" minerals may create a potential obstacle to the widespread adoption of low-carbon energy technologies. To minimize the risks, the Critical Minerals Strategy [1] recommended accelerating the growth of the UK's domestic mining capabilities, involving the development of new processing technologies for the exploitable deposits and mining tailings for the exhausted deposits. These deposits often contain economically important (up to dominant) amount of refractory form of Platinum Group Elements (PGEs) together with toxic elements, e.g. Se, As, Tl.

The solubility of Pt/Pd in natural pyrite FeS_2, one of the ubiquitous minerals in sulphide deposits, can reach a few hundred ppm [2,3]. At the same time, many studies report on the close spatial distribution of "critical" metals Pt/Pd and toxic Se in pyrite grains [4,5]. Our recent investigation aims to study the nature of Pt-Se and Pd-Se substitutions in pyrite [6].

Pyrites were obtained under anoxic conditions via the salt flux method of synthesis. The grains contained (i) 3.8 wt% of Se and 0.2 wt% of Pt, (ii) 1.1 wt% of Se and 0.3 wt% of Pt, and (iii) 1.5 wt% of Se and 0.7 wt% of Pd.

Se-doped crystals were studied by X-ray absorption spectroscopy XANES/EXAFS* in fluorescence mode at the Se K-edge to reveal the oxidation state and the local atomic environment of Se [6]. All the collected XANES spectra are similar (Fig. 18) independently of the presence of the second admixture (Pt/Pd) indicating the absence of clustering of Pt/Pd and Se. The comparison of the experimental spectra with the standards recorded in this study and those from the literature [7] reveals that the "formal" oxidation state of Se in pyrite is close to 0. The preliminary EXAFS spectra analysis demonstrated that Se predominantly replaces S in the pyrite structure. In general, the first coordination shell of the absorbing atom expands in comparison with the pure structure of pyrite. The distances to the rest of the coordination shells are close to the original distances between S and neighbouring atoms (Fig. 19) in the pure pyrite structure [8]. However, the expansion of the first coordination shell can be accounted for by the presence of the second minor form of Se: Se-Se clustering in the pyrite structure with Se content exceeding 1 wt%. Neither Pt nor Pd was detected in the Se vicinity in the pyrite structure. Hence, the presence of Pt-Se and Pd-Se clustering was ruled out. The coupled Pt-Se and Pd-Se enrichment often observed in natural pyrites may take place simultaneously, or Se changes the parameters of the pyrite unit cell which favours Pt and Pd incorporation. This result can be tested via microdiffraction measurements of the crystals.

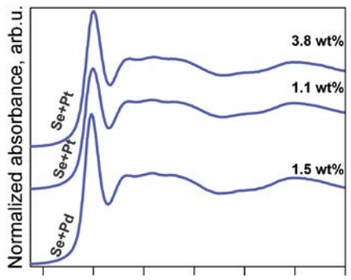

Fig. 18: Normalised Se K-edge XANES spectra of Pt-Pd-substituted pyrites.

Our findings may contribute to developing more efficient methods for extracting "critical" Pt and Pd from Se-rich pyrite, ensuring sustainable recovery while mitigating risks of toxic selenium contamination.

[1] Resilience for the Future: The UK's Critical Minerals Strategy - GOV.UK (www.gov.uk)
[2] V.A. Yakovleva *et al.*, Mineral. Mag. 67(2), 355 (2003).
[3] A. Manceau *et al.*, ACS Earth Space Chem. 4(3), 379 (2020).
[4] B.M. Boucher *et al.*, Frontiers in Earth Science. 11, 819129 (2023).
[5] R. Piña *et al.*, Miner. Deposita. 51(7), 853 (2016).
[6] O. Filimonova, expt. BM28/XMaS, A28-1-1369.
[7] A.L. Ryser *et al.*, Geochem. Trans. 6(1), 1 (2005).
[8] G. Brostigen *et al.*, Acta Chem. Scand. 23(6), 2186 (1969).

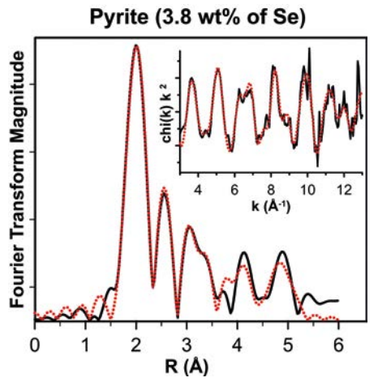

Fig. 19: The k^2-weighted background-subtracted Se K-edge EXAFS spectrum (insert) together with its Fourier transform (not corrected for phase shift; black line – experiment, dotted red line – simulation).

XANES: X-Ray Absorption Near Edge Spectroscopy. EXAFS: Extended X-ray Absorption Fine Structure.

For more information, contact
O.N. Filimonova, Department of Physics, University of Liverpool, UK
olga.filimonova@esrf.fr

ACCESS TO SYNCHROTRON and OFFLINE FACILITIES

Two proposal review rounds are held each year. **Deadlines for applications to make use of the National Research Facility (CRG) time are normally 1st April and 1st October** for the scheduling periods August to February and March to July, respectively.

Applications for beamtime must be submitted electronically via the ESRF web page: www.esrf.eu. Select **"Users & Science"**, then choose **"Applying for beamtime"** from the drop-down list. On the right hand side, you can consult the instructions to submit your proposal and access the **"User Portal"**. Enter your surname and password and select **"Proposals/Experiments"**. Follow the instructions carefully — you must choose **"CRG Proposal"** and **"BM28 (XMaS - Mat.Sci.)"** at the appropriate stage in the process. If you experience any problems, please contact Laurence Bouchenoire (bouchenoire@esrf.fr). Technical specifications and instrumentation available are described on the XMaS web page (www.xmas.ac.uk). All sections of the form must be filled in. Particular attention should be given to the safety aspects with the name and characteristics of your samples completed carefully. Experiments requiring special safety precautions such as the use of electric fields, lasers, high pressure cells, dangerous substances, toxic substances and radioactive materials, must be stated clearly in the proposal. Moreover, any ancillary equipment supplied by the user must conform to the appropriate French regulations. Further information may be obtained from Martine Moroni, the ESRF Experimental Safety Officer for CRG beamlines (martine.moroni@esrf.fr, tel: +33 4 76 88 23 69). Please indicate your date preferences, including any dates that you would be unable to attend if invited for an experiment. This will help us to produce a schedule that is satisfactory for all.
When preparing your application, please consider that access to the National Research Facility is reserved for UK based researchers. Collaborations with EU and international colleagues are encouraged, but the proposal must be led by a UK based principal investigator. It must be made clear how any collaborative research supports the wider UK science base. Applications without a robust link to the UK will be rejected and should instead be submitted directly to the ESRF using their public access route.
Access to the XMaS beamline is also available for one third of its operational time to the ESRF's user community. Applications for beamtime within that quota should be made in the **ESRF's proposal rounds (application deadlines 4st March and 10th September)**. Applications for the same experiment may be made to both XMaS directly and to the ESRF. Obviously, proposals successfully awarded beamtime by the ESRF will not then be given additional time in the XMaS allocation.
An experimental report on completed experiments must be submitted electronically, following the ESRF model. The procedure for submitting experimental reports follows that for the submission of proposals. Please follow the instructions on the ESRF's web pages carefully. **Reports must be submitted within 6 months of the experiment.** Note that the abstract of a publication can also serve as the experimental report! Please also remember to fill in the XMaS end of run survey form on completion of your experiment, which is available on the website (https://bit.ly/3JM6E7q).

Assessment of Applications
The independent Peer Review Panel considers the proposals, grades them according to scientific excellence, adjusts the requested beam time if required, and recommends proposals to be allocated beam time on the beamline. Experimental reports will also form part of the assessment criterion. Proposals which are allocated beamtime must meet ESRF safety and XMaS technical feasibility requirements. Following each meeting of the Peer Review Panel, proposers will be informed of the decisions taken and feedback provided.

APPLICATIONS FOR OFFLINE FACILITY TIME

Submit your application directly on the XMaS web site: www.xmas.ac.uk. Select **"XMaS Offline Facilities"** and then **"Application for Offline Facilities"**. Follow the instructions carefully and do not forget to upload your 1-2 page proposal at the end of the application form. Please contact the local staff to discuss any potential experiments. Successful offline proposals will be run as in-house experiments. We will complete the safety form with the information supplied in your application form as well as arrange site passes and any accommodation that may be required. As for synchrotron beamtime, offline users normally stay in the ESRF guest house or off-site hotels.

The XMaS facility implements transparent policies and procedures to guarantee that access is based on scientific excellence only. In partnership with the ESRF Safety office, we will endeavor to ensure that the facility can accommodate any user, but this may require an individual needs assessment. If you have any questions about accessing the facility at any stage of the application or experimental processes, please do not hesitate to get in touch.

Living allowances
These are €90 per day per beamline user — the equivalent actually reimbursed in sterling. XMaS will support up to 3 users per synchrotron experiment and only 1 on the offline laboratories. For experiments which are user intensive, additional support may be available. The ESRF hostel still appears adequate to accommodate all our users, though CRG users will always have a lower priority than the ESRF's own users. Do remember to complete the "A-form" when requested to by the ESRF, as this is used for hostel bookings, site passes and to inform the safety group of attendees.

Beamline people

ONSITE TEAM

Didier Wermeille
didier.wermeille@esrf.fr
is the Beamline Responsible who, in partnership with the Directors, oversees the activities of the user communities as well as the programmes and developments that are performed on the beamline. He is also the beamline Safety Representative. His expertise spans crystallography, high resolution diffraction, surface studies, magnetic scattering and electric field measurements.

Laurence Bouchenoire
bouchenoire@esrf.fr is the Beamline Coordinator. She looks after beamline operations and can provide you with information about the beamline, application procedures, scheduling, etc. Laurence should normally be your first point of contact. Her expertise is in magnetic scattering including polarisation dependence.

Oier Bikondoa
oier.bikondoa@esrf.fr
is Beamline Scientist with expertise in soft matter materials, (GI-)SAXS/WAXS, surface and reflectivity studies.

Olga Filimonova
olga.filimonova@esrf.fr is our PDRA with expertise in spectroscopy.

Paul Thompson
pthompso@esrf.fr is the contact for instrument development, technical support, sample environments including electric field, liquid cells and catalysis.

PROJECT DIRECTORS

Chris Lucas clucas@liv.ac.uk and **Tom Hase** t.p.a.hase@warwick.ac.uk continue to travel between the UK and France to oversee the operation of the beamline.

Malcolm Cooper
m.j.cooper@warwick.ac.uk
remains involved in the beamline operation as an Emeritus Professor at the University of Warwick.

Yvonne Grunder
yvonne.grunder@liverpool.ac.uk
is part of the management team at Liverpool to provide additional support. She also oversees impact activities.

Julie Clark
Julie.Clark@liverpool.ac.uk
is the administrator on the project, based in the Department of Physics at Liverpool.

THE PROJECT MANAGEMENT COMMITTEE

The current membership of the committee is as follows:
C. Nicklin (chair), DLS
L. Behrooz, EPSRC
M. Alfredsson, Uni. of Kent
M. Cain, Electrosciences Ltd
A. Beale, Uni. College London
K. Edler, Uni. of Bath
B. Hickey, Uni. of Leeds
S. Langridge, ISIS
W. Stirling, Institut Laue Langevin

In addition to the above, the directors, the chair of the Peer Review Panel, the CRG Liaison M. Hahn and the beamline team are in attendance at the meetings which happen twice a year.

THE PEER REVIEW PANEL

The current membership of the panel is as follows:
R. Arrigo (chair), Uni. of Salford
A. Hector, Uni. of Southampton
E. Heeley, Open University
M. Skoda, ISIS
K. Syres, Uni. of Central Lancashire
L. Ishibe-Veiga, DLS
M. Senn, Uni. of Warwick.

In addition, either Chris Lucas or Tom Hase attends their meetings in an advisory role.

PUBLISH PLEASE!!... and keep us informed

One of the important XMaS KPIs is the number and quality of publications. We ask you to provide us (xmas@esrf.fr) with the reference and DOI whenever a new paper is published. Alternatively, you can submit your new publication reference directly through a form on our web site (https://bit.ly/2Gja4zX). Please also let us know about other impact generated as a result of XMaS work.

IMPORTANT!
It is important that we acknowledge the support from EPSRC in any publications. When beamline staff have made a significant contribution to your scientific investigation you may naturally want to include them as authors. Otherwise we ask that you add an acknowledgement of the form:

"XMaS is a UK national research facility supported by EPSRC. We are grateful to all the beamline staff for their support."

Editor: Laurence Bouchenoire - Graphic Designer: Sylvie Quercia - Print: Warwick Print - February 2024

XMaS (BM28)
the UK Materials Science Beamline

ESRF - The European Synchrotron
71 avenue des Martyrs, CS 40220
38043 Grenoble Cedex 9,
France

Tel: +33 (0)4.76.88.25.80
xmas@esrf.fr

@XMaSBeam

www.xmas.ac.uk

XMaS the UK-CRG

UNIVERSITY OF LIVERPOOL

UKRI Engineering and Physical Sciences Research Council

WARWICK
THE UNIVERSITY OF WARWICK